Stable Gene Transfer to Muscle Using Non-integrating Lentiviral Vectors

Luis Apolonia[1,2,3], Simon N Waddington[4], Carolina Fernandes[1,2], Natalie J Ward[1,2], Gerben Bouma[1,2], Michael P Blundell[1,2], Adrian J Thrasher[1,2], Mary K Collins[3] and Nicola J Philpott[1,2]

[1]Molecular Immunology Unit, Institute of Child Health, London, UK, [2]Great Ormond Street for Hospital NHS Trust, London, UK; [3]Department of Immunology and Molecular Pathology, Windeyer Institute, University College London, UK; [4]Department of Haematology, Haemophilia Centre and Haemostasis Unit, Royal Free and University College Medical School, London, UK

Human immunodeficiency virus (HIV)-based lentiviral vectors (LVs) hold immense promise for gene delivery applications because of their relatively large packaging capacity and their ability to infect a range of cell types. The genome of HIV non-specifically integrates into the host genome, and this promotes efficient, stable transgene expression in dividing cells. However, integration can also be problematic because of variations in gene expression among cells, possible gene silencing and, most importantly, insertional mutagenesis which can lead to undesirable effects such as malignant transformation. In order to alleviate these problems, we have developed a range of non-integrating LVs (NILVs) by introducing point mutations into the catalytic site, chromosome binding site, and viral DNA binding site of the viral integrase (IN). In addition, we have mutated the IN attachment (att) sites within the HIV long terminal repeats (LTRs). All of the vectors produced show efficient reverse transcription and transgene expression in dividing cells and prolonged expression in non-dividing myotubes. Finally, we show that NILV can be used for achieving highly effective gene transfer and expression in muscle *in vivo*.

Received 9 February 2007; accepted 16 July 2007; published online 14 August 2007. doi:10.1038/sj.mt.6300281

INTRODUCTION

Lentiviruses such as human immunodeficiency virus (HIV) are effective tools for gene transfer to a range of cell types including post-mitotic cells.[1] The efficient transduction achieved by using lentiviruses as genetic vectors is partly because of their ability to integrate into the genome. However, an integrated transgene is differentially expressed among cells, and insertion of a transgene in the vicinity of an oncogene or tumor suppressor gene can cause malignant transformation.[2,3] We have recently demonstrated that non-integrating LVs (NILVs) can be used as effective tools for gene therapy.[4] They effectively transduce cells by harnessing active transcription from the episomal forms of the viral genome. These viral episomes are diluted through cell division, so that NILVs can be used for achieving transient expression of a transgene in dividing cells.[5] Alternatively, NILVs have a wide range of potential use in gene transfer to post-mitotic tissue where the episomal genome is not diluted through cell division. Therefore, by eliminating integration and minimizing the risk of insertional mutagenesis, NILVs may be safer than integrating vectors in the treatment of genetic disease in post-mitotic tissue.

The development of NILVs relies upon the production of the double-stranded viral DNA molecule which must be transcribed to allow efficient expression of the transgene. Accordingly, vector production and entry into the host cell must not be disrupted, and the vector genome should undergo effective reverse transcription and nuclear entry. The product of reverse transcription is a linear blunt-ended double-stranded DNA molecule which is the substrate for viral integration.[6,7] Importantly, circular DNA molecules are also created from the linear DNA as by-products of integration.[8–11] These episomes are actively transcribed and accumulate in cells infected with NILVs.[12–15] DNA circles containing one long terminal repeat (LTR) form by homologous recombination between the two viral LTRs; circular viral DNA containing two LTRs are thought to be produced from non-homologous end-joining of the LTRs.[16–19]

HIV-1 integration is mediated by the 32 kd viral integrase (IN) which is encoded by the *pol* gene. IN functions by binding to the U3 and U5 attachment (att) sites within the LTRs of the viral DNA and mediating its integration into the host genome.[20,21] For the development of NILVs, IN cannot be deleted completely because it is involved in reverse transcription and nuclear import of the pre-integration complex.[22,23] However, integration can be blocked by introducing point mutations into IN or by mutating the att sites in the viral DNA.[5,20,21,24–27] HIV-1 IN mutations can be divided into two classes. Class I mutations result in the vector being defective specifically for integration, whereas class II mutants display additional assembly or reverse transcription defects that result in a lack of integration.[28] Therefore, in order to develop NILVs that express a transgene from the episomal DNA, we have focused on introducing class I mutations.

In this study we inhibited LV integration by different methods. First, by introducing mutations into IN at positions D64, N120,

Correspondence: *Nicola J. Philpott, Molecular Immunology Unit, Institute of Child Health, 30 Guilford Street, London WC1N 1EH, UK. E-mail: n.philpott@ich.ucl.ac.uk*

W235, Q148, K264, K266, and K273; and second, by mutating the IN att sites within the viral LTRs. We present green fluorescent protein (GFP) expression data showing that all of the vectors were able to transduce cells efficiently *in vitro*. In contrast to dividing cells, that showed only transient expression, non-dividing myoblasts were found to retain transgene DNA *in vitro*, and expression from the transgene was stable for the duration of the experiments. Furthermore, we show that HIV-based NILVs can be used to transduce muscle efficiently *in vivo,* and that prolonged transgene expression can be achieved.

RESULTS

Analysis of mutant vectors

The main objective of this study was to determine whether LVs containing various integration mutations could function as efficiently as their integrating counterparts in post-mitotic tissue. All of the mutants developed were selected based on previous studies which showed their ability to specifically inhibit integration, and thereby retain the transducing activity of the virus. Two approaches were taken to prevent integration. The first was to introduce class I point mutations into IN at positions D64, N120, Q148, and W235 (**Figure 1a**). Residue Q148 is involved in binding to the viral DNA,[29,30] and amino acids N120 and W235 are critical for binding to the chromosomal target DNA.[24,31] The D64 residue was mutated because it is part of the DDE catalytic triad that is absolutely essential for integration.[24] The requirement for amino acids K264, K266, and K273 in integration has been the subject of recent debate.[25,32] We mutated these lysines to arginine residues for assessing their integration efficiency and long-term transgene expression. The second method of blocking integration was to mutate the IN att sites in the vector genome by replacing the conserved CA dinucleotides with TG residues (**Figure 1b**).[5,20,21,27] Furthermore, in order to improve safety and to determine whether the various mutations could function synergistically, vectors containing multiple mutations were generated.

To confirm that introduction of the various mutations in IN (D64V, N120L, Q148A, W235E, K264,266,273R) and in the IN att sites did not interfere with virus production, the concentration

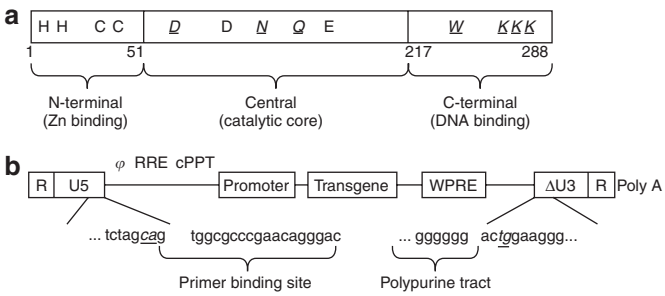

Figure 1 Schematic illustration of the mutations created in integrase and in the viral genome. (**a**) Integrase domains: bold font represents conserved amino acids [Zinc (Zn) finger (HHCC) and catalytic core (DD(35)E), mutated residues are underlined. (**b**) Viral genome showing conserved ca (attachment sites); underlined ca and tg show where mutations were introduced. cPPT, central polypurine track; RRE, Rev responsive element; WPRE, woodchuck hepatitis virus post-transcriptional regulatory element.

of p24 was measured. The p24 enzyme-linked immunosorbent assay (ELISA) results in **Table 1** show little variation between the different vector stocks indicating that introduction of the class I IN mutations or att site mutations (Δatt) did not interfere with virus budding and production. Viral titer was quantified by measuring transducing units in 293T cells. **Table 1** shows high titer for the virus generated from all of the vector preparations. To quantify the level of transgene expression, the mean fluorescence intensity of enhanced GFP (eGFP) was measured in cells infected by the mutant vectors. As shown in **Table 1**, the IN and att site mutations have minimal effect on the mean fluorescence intensity. It follows, therefore, that the IN and att site mutations that we introduced allow efficient viral genome encapsidation, reverse transcription of the RNA genome, nuclear entry of the viral complementary DNA, and efficient transcription and translation of the transgene.

Mutant vectors are integration-deficient

In order to evaluate transgene expression over time, 293T cells were transduced by vectors at the same multiplicity of infection (0.3, to ensure low starting vector copy numbers), and eGFP expression was measured by flow cytometry. All of the vectors containing IN or att site mutations show a decrease in eGFP expression over time (**Figure 2**). By 14 days after transduction, background levels of expression were seen in cells transduced by the D64V, N120L, W235E, and Δatt vectors, as well as by the vectors containing multiple mutations. Cells transduced by the

Table 1 Characterization of enhanced green fluorescent protein-expressing vectors: quantification of p24 and eGFP expression levels *in vitro*

Virus	Viral particles (pg p24/ml)[a]	Titer (TU/ml)[b]	MFI[c]
Wt	2.89E + 07	1.09E + 09	1.00
D64V	3.12E + 07	4.41E + 08	0.47
N120L	2.47E + 07	5.50E + 08	0.53
W235E	1.98E + 07	2.12E + 08	0.59
Q148A	2.59E + 07	2.87E + 08	0.72
K264R	1.46E + 07	2.60E + 08	0.84
K264,266,273R	1.28E + 07	3.67E + 08	0.75
D64V + N120L	4.21E + 07	3.63E + 08	0.52
D64V + W235E	4.72E + 07	3.11E + 08	0.59
D64V + N120L + W235E	3.91E + 07	4.91E + 08	0.70
Δatt	2.53E + 07	5.01E + 08	0.75
D64V + Δatt	5.24E + 07	2.68E + 08	0.80
D64V + N120L + W235E + Δatt	6.35E + 07	4.18E + 08	0.66

Titer measurements were obtained from serial dilutions of at least three separate batches of each vector.
[a]Quantification of p24 concentration in viral stocks, measured by performing a p24 enzyme-linked immunosorbent assay using serial dilutions of the vectors. [b]Titer: 293T cells were infected with serial dilutions of vectors expressing enhanced green fluorescent protein (eGFP). Flow cytometry was performed on the second day after infection and titers were calculated in transducing units/ml (TU). [c]Mean fluorescence intensity (MFI): 293T cells were infected at the same multiplicity of infection (0.3). Expression levels were measured by flow cytometry at 2 days after infection. The MFI values obtained for the mutant vectors were normalized to the MFI of cells infected by the vector containing wild-type (wt) integrase and attachment sites, which was given a value of 1.00.

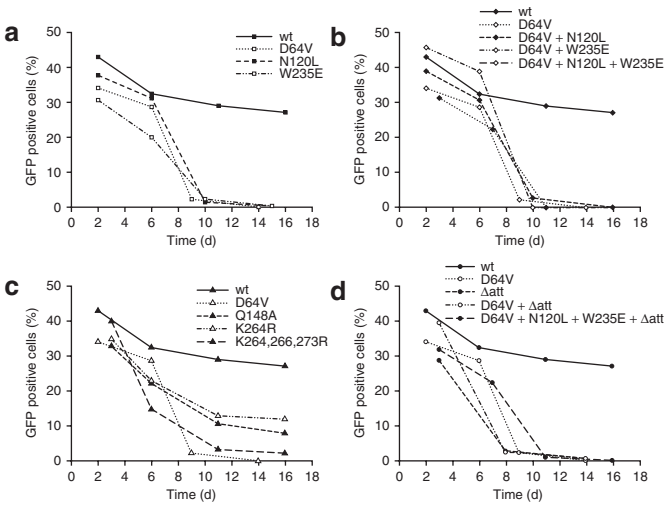

Figure 2 Transgene expression profile of cells infected with the vectors. 293T cells were infected with vectors expressing enhanced green fluorescent protein (eGFP) at multiplicity of infection 0.3. The percentage of transgene-expressing cells was monitored over time by flow cytometry. For easy comparison, wild-type (wt) and D64V vectors are shown on all graphs. (**a**) Cells infected with N120L and W235E vectors; (**b**) cells infected with vectors containing multiple mutations: D64V + N120L, D64V + W235E, and D64V + N120L + W235E; (**c**) cells infected with wt, D64V, Q148A, K264R, and K264,266,273R mutant vectors; (**d**) cells infected with vectors containing a combination of mutant integrase and mutant attachment sites: Δatt, D64V + Δatt and D64V + N120L + W235E + Δatt (DNWΔatt). The graphs shown are representative of at least three separate experiments using different batches of each vector.

Q148A, K264R, and K264,266,273R vectors also lost some eGFP expression over time, but expression reached a plateau by 11 days after transduction. At 2 weeks after transduction, the K264R, Q148A, and K264,266,273R vectors had 1.5-fold, 2-fold, and 5-fold lower expression levels than the vector with wild-type (wt) IN, respectively. This indicates that, although these mutants do cause impairment of integration, they do not block integration as efficiently as the D64V, N120L, W235E, or Δatt mutations. In summary, we have demonstrated that all of the mutant vectors are able to transduce cells. However, expression of the transgene is lost over time in dividing cells because of a lack of viral DNA integration into the host cell genome.

Quantification of background integration

Data obtained from measuring eGFP expression in 293T cells suggested that all of the mutant vectors were integration-deficient. Next, we wanted to quantify more precisely the efficiency of residual integration. The level of background integration of the class I mutants was calculated by infecting HT1080 cells with vectors expressing a neomycin resistance gene (*Neo*) at a multiplicity of infection of 0.3. Cells were selected over a period of 3 weeks, and the number of G418-resistant colonies gave a defined level of residual integration. This level was compared with the integration efficiency of the vector containing wt IN.

As shown in **Figure 3**, the level of background integration of the D64V, N120L, and W235E mutants is 10^3-fold lower than integration of the wt vector. The residual integration rate of the K264R, Q148A, and K264,266,273R mutants was higher, being 3-, 13- and 14-fold lower than with the wt vector, respectively.

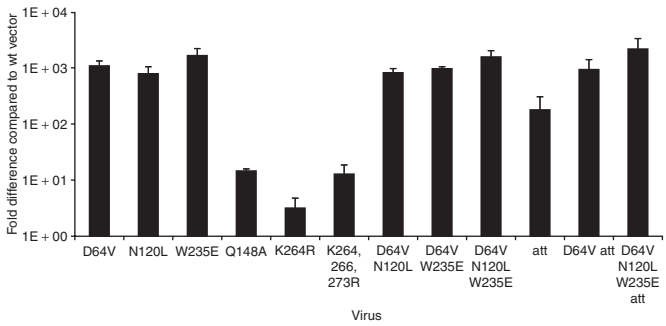

Figure 3 Quantification of background integration of mutant vectors. Vectors were standardized according to concentration of p24. HT1080 cells were infected with serial dilutions of vectors expressing a neomycin resistance gene. Colonies were counted after 3 weeks of incubation in medium supplemented with G418. Integration efficiency was calculated by comparing the number of colonies on plates transduced by mutant vector with the number of colonies on plates transduced by vector containing wild-type (wt) integrase. The differences in integration levels represent the level of integration inhibition caused by the various mutations. The error bars represent the SD calculated from at least three separate infections of each vector. att, attachment sites.

The higher background integration seen with the K264R, Q148A, and K264,266,273R Neo vectors in HT1080 cells correlates with the plateau of eGFP expression seen in 293T cells 11 days after infection (**Figure 2**). Taken together, these results suggest that mutations K264R, Q148A, and K264,266,273R are not as effective at blocking integration as the D64V, N120L, and W235E IN mutations.

Mutation of both IN att sites in the viral genome also inhibited integration. The integration efficiency of the Δatt mutant was 200-fold lower than that of the vector containing wt att sites. Interestingly, inserting a combination of mutations into IN and the att sites appeared to have little affect on lowering the level of residual integration beyond that seen with the D64V mutant. These results imply that introduction of multiple class I IN or att site mutations does not have a synergistic or additive effect on the level of background integration.

Efficient transgene expression in non-dividing cells

Our goal was to further analyze various NILVs for their use as gene therapy vectors for delivery to post-mitotic tissue. Therefore, in order to assess their performance *in vitro,* we investigated the kinetics of viral expression in non-dividing cells, using C2C12 muscle cells as a model. The C2C12 cells were infected with the integration mutants and allowed to terminally differentiate into myotubes by serum starvation. eGFP expression was then monitored over time. As shown in **Figure 4**, the expression of eGFP in dividing C2C12 cells decreased after 5 days following infection for all of the mutant vectors, and this correlates with the transient expression seen in 293T cells (**Figure 2**). Conversely, in non-dividing C2C12 myotubes, transgene expression was stably maintained for all of the vectors. Expression from the NILVs was similar to expression from the integrating vector for at least 12 days after infection (the life-span of the myotubes, and therefore the duration of the experiment).

We also investigated the viral DNA in non-dividing C2C12 myotubes at two different time points (3 and 12 days after

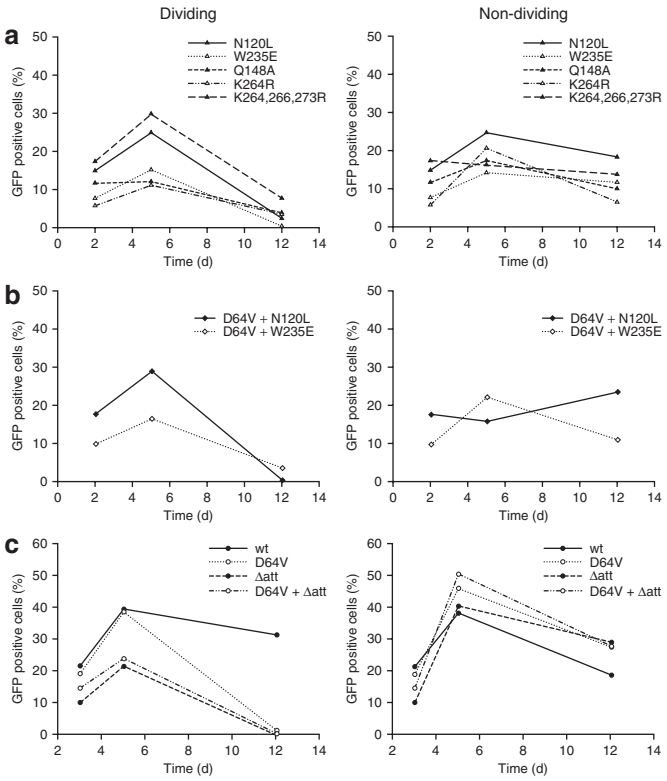

Figure 4 Expression profile in non-dividing cells. C2C12 myoblast cells were infected with vectors expressing enhanced green fluorescent protein (eGFP) at multiplicity of infection 10. Transgene expression was measured over time by flow cytometry. Differentiation was induced using medium containing 2% horse serum, thereby arresting cell division at 3 days after transduction. Graphs on the left represent dividing C2C12 cells and those on the right represent differentiated non-dividing C2C12 cells. (**a**) Cells infected with vectors harboring integrase (IN) mutations N120L, W235E, Q148A, K264R, and K264,266,273R; (**b**) Cells infected with vectors containing multiple IN mutations D64V + N120L and D64V + W235E; (**c**) Cells infected with wild-type (wt) vector, the catalytic mutant D64V, the attachment site mutant (Δatt), and the combination of D64V and Δatt. The graphs shown are representative of at least two separate experiments using different batches of each vector.

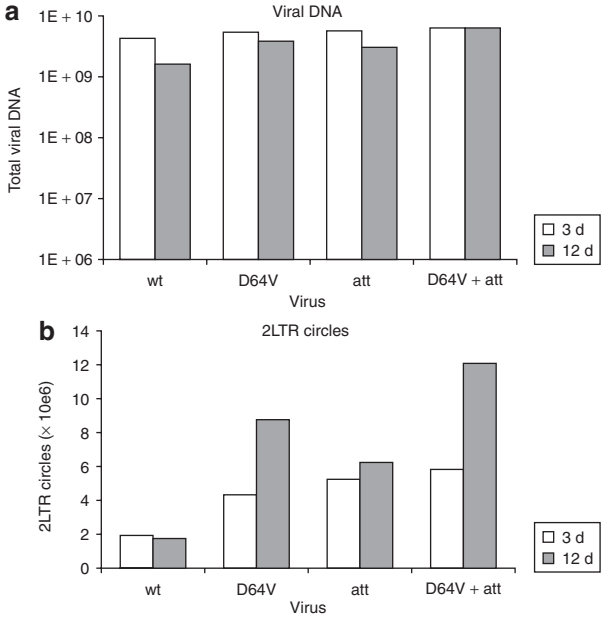

Figure 5 Viral DNA characterization in non-dividing C2C12 cells. C2C12 cells were infected at multiplicity of infection 10 and growth was arrested in medium containing 2% horse serum. Total DNA was harvested at 3 and 12 days after infection. (**a**) Total viral DNA and (**b**) 2LTR viral DNA circles were quantified by quantitative polymerase chain reaction. Serial dilutions of plasmid DNA containing the relevant sequence were used as standards (see Materials and Methods). LTR, long terminal repeat. att, attachment sites.

infection). **Figure 5a** shows that at 3 days after infection the level of total viral DNA was similar in cells infected by all of the vectors tested (wt IN, D64V, Δatt, and D64VΔatt). Importantly, the viral DNA was not degraded over time, and the levels were maintained to the later time point of 12 days after infection (**Figure 5a**). This correlates with the persistence of eGFP expression seen in non-dividing C2C12 myotubes (**Figure 4**). Because the viral DNA in cells infected by mutant vectors is not integrated, we quantified the level of extrachromosomal DNA in the C2C12 myotubes by measuring the level of 2LTR circles using quantitative polymerase chain reaction (**Figure 5b**). The level of 2LTR viral DNA circles increased over time in myotubes infected with the D64V IN mutant. This contrasted with myotubes infected by vector containing wt IN which retained a constant level of 2LTR circles. By 12 days after infection, the myotubes infected by any of the three mutants contained higher levels of 2LTR circles than those of the wt vector. Specifically, the D64V, Δatt, and D64VΔatt mutants generated fivefold, fourfold and sevenfold more 2LTR circles than wt vector, respectively. This increase in 2LTR circles over time confirms that the extrachromosomal DNA is not degraded in non-dividing myotubes. Furthermore, it also suggests that by inhibiting integration the viral DNA is accessible to undergo circularization within the myotube, resulting in an accumulation of circular episomal genomes.

Efficient transgene expression *in vivo*

The *in vitro* integration efficiency analysis indicated that the D64V, N120L, W235E, and Δatt mutations produced lower residual integration than the other mutants (**Figure 3**). We therefore combined these mutations and assessed transduction efficiency in muscle *in vivo*. The D64V, Δatt, D64VΔatt, and DNWΔatt mutant vectors were compared with integrating vector expressing eGFP. The vectors were injected intramuscularly into neonatal mice. At 1 month after injection, muscle samples were sectioned and eGFP was visualized by immunohistochemical staining (**Figure 6a**). At 3 months after injection eGFP was visualized in whole legs, under a fluorescence microscope (**Figure 6b**). Transgene expression was detected in all the samples injected with the mutant vectors, thereby indicating that NILVs can mediate long-term transgene expression in muscle tissue *in vivo*. These results correlate well with the prolonged expression observed in C2C12 non-dividing myotubes (**Figure 4**). eGFP expression in the muscle was quantified by ELISA and compared with levels of residual eGFP in the vector stocks (**Supplementary Table S1**). The ELISA results confirm that eGFP was expressed in muscle *in vivo*. Furthermore, the integrating vectors and NILVs mediated similar levels of transgene expression ($P > 0.05$ by Kruskal–Wallis test) (**Figure 6c**). Finally, the formation of viral 2LTR circles was measured from the

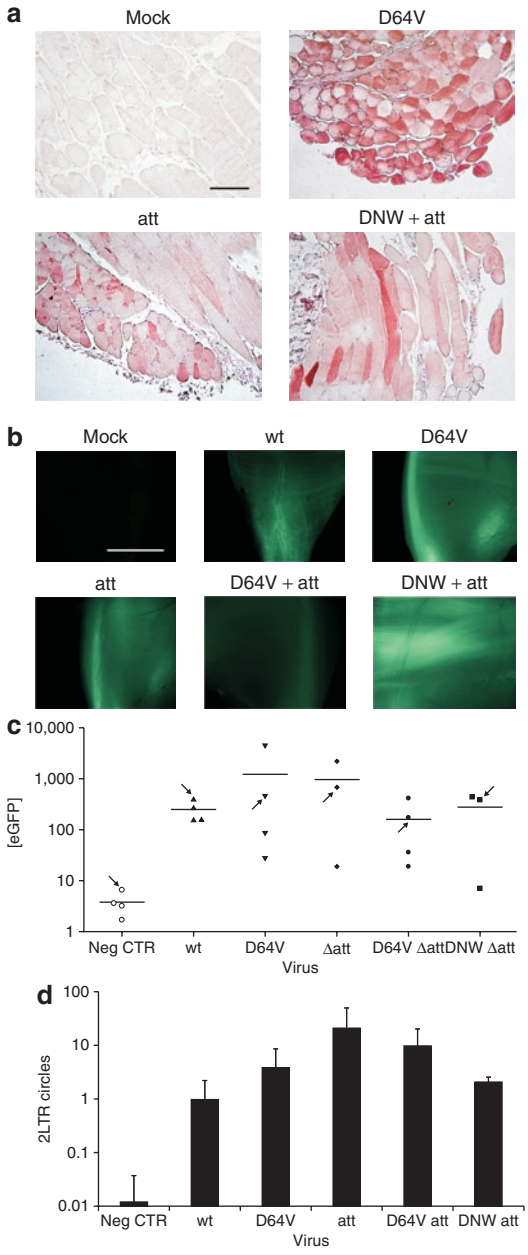

Figure 6 Transgene expression in muscle *in vivo*. Vectors were injected intramuscularly into 1-day-old mice using 5 µl of each vector per mouse. (**a**) Photographs of tibialis anterior muscle sections taken at 1 month after injection. Intracellular enhanced green fluorescent protein (eGFP) is stained with 3-amino-9-ethylcarbazole (red), scale bar = 100 µm. One representative photograph of at least five replicates is shown. (**b**) eGFP expression was visualized in whole legs under a fluorescence microscope at 3 months after injection. We show one representative photograph of at least three replicates for each virus injected, scale bar = 3 mm. (**c**) Quantification of eGFP from *in vivo* muscle samples 3 months after injection. Total protein was extracted from 20 mg of muscle at 3 months after injection. eGFP was quantified by enzyme-linked immunosorbent assay alongside a commercial eGFP standard (Clontech). Values were standardized to total protein using a Bradford assay. Values represent picograms of eGFP per microgram of total protein. Each dot represents one mouse and the arrows indicate the legs shown in **Figure 6a**. (**d**) Total DNA was extracted from muscle samples at 3 months after injection and used as a template to quantify the level of 2LTR viral DNA circles by quantitative polymerase chain reaction (see Materials and Methods). LTR, long terminal repeat.

3-month muscle samples. **Figure 6d** shows that all of the vectors efficiently transduced muscle, and that the viral genomes were reverse transcribed and entered the nucleus where viral DNA circularization occurred.

Taken together, the results presented in **Figure 6** suggest that introduction of the class I IN and att site mutations did not interfere with LV transduction. Furthermore, the level of eGFP expression from NILVs was comparable to expression from the integrating vector in muscle *in vivo*.

DISCUSSION

Recently there has been a lot of interest in the development of integration-deficient LVs for safer gene therapy. These vectors utilize the high transduction efficiency and broad tropism of lentivirus but avoid the potential problems associated with the non-specific integration of a transgene.[2] NILVs are defective specifically for integration, so that earlier steps in the viral life cycle are not compromised and efficient cell transduction can still be achieved. NILVs will be particularly useful in non-dividing cells because the vector genome is not diluted through cell division. Efficient transgene expression has previously been achieved in ocular and brain tissues of rodents.[4,33] In this study we have directly compared various integration mutants by characterizing their ability to deliver a transgene efficiently and stably to non-dividing cells in culture. Furthermore, we have extended the potential therapeutic repertoire of NILVs by achieving prolonged transgene expression in muscle *in vivo*.

The IN and IN att site mutations used in our study have all previously been shown to specifically inhibit the integration step of the lentivirus life cycle.[5,20,21,24–27] We were able to produce vectors containing the mutations to high titer, and our initial experiments confirmed that introduction of these mutations did not interfere with virus production, reverse transcription, nuclear entry or transgene expression (**Table 1**). Subsequently we found that the mutant vectors exhibited transient expression in dividing cells, thereby implying that the vectors were indeed defective for integration (**Figure 2**).

We extended this work by directly comparing the integration efficiency of each vector (**Figure 3**). The D64V, N120L, and W235E vectors integrated approximately 10^3-fold less frequently than the vector containing the wt IN. Leavitt and colleagues found that a vector with an N120L point mutation integrated 3 log units less efficiently; and vectors with D64V and W235E mutations integrated 4 log units less efficiently, than wt vector.[24] Q148A was a less effective mutation, and its integration efficiency was closer to wt levels. Mutation of the C-terminal lysines at positions 264, 266, and 273 reduced integration efficiency by 1 log unit, thereby suggesting that these residues are required for optimal IN function; this correlates with results from the work by Cereseto *et al.*[25] However the presence of lysine residues is not absolutely essential for HIV integration, as was shown in a recent study by Topper and colleagues.[32] Our Δatt vector integrated 200-fold less efficiently than wt; this correlates with results by Masuda and coworkers, who found that mutating both att sites decreased integration to 1% of wt levels.[20]

In an attempt to further decrease residual integration and thereby reduce the risk of insertional mutagenesis, we developed

vectors containing multiple integration mutations. However, upon analysis we found that introducing a combination of mutations had no effect on reducing integration efficiency. Nightingale *et al.* used a D64V/att site double mutant and found that there was no further reduction in integration efficiency beyond that of the D64V mutation alone. Subsequent integration site analysis suggested that the residual integration of the D64V mutant was not mediated by IN but by cellular recombination events.[5] Therefore it appears that integration of LVs cannot be inhibited to levels more than 10^4-fold lower than wt levels in the presence of antibiotic selection. However, in order to minimize the potential risk of reversion to an integrating phenotype, it may be prudent to generate vectors with multiple IN mutations for clinical application.

Our studies as well as those of others have recently shown that expression from NILVs can persist in post-mitotic retinal and brain tissue.[4,33] In order to extend the repertoire of cells that are amenable to stable transduction by NILVs, we monitored long-term expression in muscle cells. Initially C2C12 cells were examined *in vitro*. As expected, we found that dividing C2C12 cells lost transgene expression over time (**Figure 4**), in a manner similar to the decrease observed in 293T cells (**Figure 2**). Previously Vargas *et al.* had shown that it is possible to prolong transgene expression in dividing cells by incorporating an SV40 ori into the genome that mediates viral complementary DNA replication in the presence of T antigen.[34] Our approach was to induce growth arrest in the C2C12 cells so as to prevent loss of the viral genome through cell division, and this allowed persistent transgene expression for the duration of the experiment (**Figure 4**).

In order to confirm that prolonged transgene expression in the non-dividing C2C12 myotubes was due to maintenance of the episomal viral DNA, we quantified the level of 2LTR circles in the transduced cells (**Figure 5**). The concentration of episomal 2LTR DNA was higher in cells transduced by the D64V and att mutant NILVs than by their integrating counterpart. Similar results were obtained by Yanez-Munoz *et al.* who observed eightfold more 2LTR circles in eyecups of mice transduced by the D64V vector than in those transduced by the integrating vector.[4] The persistence of 2LTR circles in C2C12 cells (**Figure 5**) correlates with the observed stability of transgene expression in non-dividing cells *in vitro* (**Figure 4**). Butler and colleagues quantified the level of 1LTR and 2LTR circles in dividing cells infected with HIV-based vectors, and found a ratio of approximately 9:1.[35] Therefore our measurement of 2LTR circles alone may have led to an underestimation of the actual concentration of circular episomes. The 2LTR circles were monitored over time, and appeared to accumulate in the C2C12s transduced by the D64V and att mutant NILVs. Saenz and coworkers observed similar maintenance of circular episomes in growth arrested cells infected by D64N and D116N NILVs.[15] Terskikh *et al.* detected episomal circles from integrating LVs in many generations of mouse hematopoietic stem cells.[36] Taken together, this work suggests that the episomal viral DNA is stable, and accumulates in post-mitotic cells transduced by NILVs.

In vivo experiments involved delivery of the D64V, Δatt, D64VΔatt, and DNWΔatt NILVs into post-mitotic tibialis anterior muscle in neonatal mice.[37] Li *et al.* have previously shown that integrating LVs can stably transduce muscle *in vivo*.[38] In our experiments, eGFP expression was visualized at 3 months after injection and quantified using an eGFP ELISA, and the transduction was confirmed by measuring the level of viral 2LTR circles in the muscle samples. The results show that all of the NILVs tested were able to transduce muscle at an efficiency similar to that of the integrating vector (**Figure 6**). Although there was no significant difference in eGFP expression in muscle from the use of either integrating vector or NILVs, the level of eGFP expression from the NILVs appears more scattered than expression from the integrating vector. The variable expression may be because of low-level loss of the NILVs at early time points after neonatal injection, when muscle is still growing and undergoing cell division. This question could possibly be addressed by injecting adult mice and measuring transgene persistence from NILVs. However, the results in this study show that all of the NILVs retained eGFP expression to at least 3 months after neonatal injection, thereby implying that NILVs can be used for obtaining long-term transgene expression in muscle *in vivo*.

In summary, we generated a LV containing three mutations in IN as well as mutations at both att sites and this DNWΔatt vector was found to transduce muscle cells stably *in vivo*. The development of an efficient LV with multiple integration mutations minimizes the potential problem of reversion to an integrating phenotype, thereby minimizing the risk of insertional mutagenesis. We believe that the results of this study open up an array of possibilities for improving the safety and efficiency of therapeutic transgene delivery to post-mitotic tissues such as muscle.

MATERIALS AND METHODS

Plasmids. The LVs are based on HIV-1 and were generated from the pHR′SIN-cPPT-SEW parental construct,[39] which contains the spleen focus forming virus LTR driving eGFP expression. The LV plasmid pHR-Cp5EW was constructed by replacing the spleen focus forming virus promoter with the adeno-associated virus p5 promoter using the restriction sites *Eco*RI and *Bam*HI. The pHR-CSNeoW vector was derived from the pHR′SIN-cPPT-SEW plasmid by replacing eGFP with a neomycin resistance gene (*Neo*) using *Bam*HI and *Sbf*I restriction enzymes. The vectors are self-inactivating due to a deletion in the 3′ HIV-1 LTR,[40] so that only the internal promoter will be active in transduced cells.

The Δatt mutants were generated using the QuikChange Site-Directed Mutagenesis Kit (Stratagene, La Jolla, CA). U5Δatt was introduced using complementary oligonucleotide primers: 5′-GGAA AATCTCTAGTGGTGGCGCCCGAACAGGGACTTGAAAGCG-3′. The U3 Δatt mutation was generated using the following complementary primer sequences 5′-GCCACTTTTTAAAAGAAAAGGGGGGACCA GAAGGGCTAATTC-3′. The Δatt mutations were confirmed by sequencing.

Single amino acid mutations were introduced into IN in the packaging plasmid pCMVdR8.74[41] using the following oligonucleotide sequences: D64V 5′-CCAGGAATATGGCAGCTAGTTTGTACACATTTAGAAGG-3′; N120L 5′-GTACATACAGACAATGGCAGCCTTTTCACCAGTACT ACAGTTAAGG-3′; Q148A 5′-GGCATTCCCTACAATCCCCAAAGT GCAGGAGTAATAGAATCTATG-3′; R199C 5′-GGGTACAGTGCAG GGGAATGTATAGTAGACATAATAGC-3′; W235E 5′-GGACAGCAG AGATCCAGTTGAGAAAGGACCAGCAAAGC-3′; K264R 5′-GTAGT GCCAAGAAGAAGAGCAAAGATCATCAGGG-3′ and K264,266,273R 5′-CCAAGAAGAAGAGCAAGGATCATCAGGGATTATGGAAG ACAGATGGCAGG-3′. Mutations were confirmed by sequencing.

Cell lines and vector production. HT1080, 293T, and C2C12 cells were cultured in Dulbecco's modified Eagle's medium supplemented with 10% fetal bovine serum and antibiotics. In order to induce differentiation in C2C12 cells, the medium was replaced with Dulbecco's modified Eagle's medium containing 2% horse serum and antibiotics. C2C12 cells were growth arrested 3 days after transduction.

LVs were produced by transient transfection of vector genome plasmid, gag-pol packaging plasmid and envelope plasmid using polyethyleneimine reagent (Sigma-Aldrich, Gillingham, UK). Broad tropism was obtained by generating vectors with the G glycoprotein of vesicular stomatitis virus envelope.[42] The LVs were concentrated by ultracentrifugation for 1 hour 30 minutes at 30,000 rpm in a Sorval Discovery 100SE in a Surespin 630 rotor. The HIV p24 protein was quantified for all vectors, using the p24 ELISA kit (Cell Biolabs, San Diego, CA) and in accordance with the kit instructions. eGFP-expressing vectors were quantified by infecting 293T cells and measuring the percentage of eGFP-expressing cells by flow cytometry at 2 days after transduction. Flow cytometry was also used for quantifying eGFP persistence in transduced C2C12 cells.

Quantifying integration efficiency. The level of background integration of the various vectors was quantified by infecting 1×10^6 HT1080 with vectors expressing *Neo*. Media containing 1 mg/ml of G418 (Invivogen, Toulouse, France) was added to the cells at 3 days after infection. Cells were grown for 3 weeks and colonies from single clones were counted.

Analysis of viral DNA. Cells were infected with vectors and total DNA was extracted at 48 hours using a standard salting-out method.[43] Total viral DNA and 2LTR circles were quantified in triplicate by quantitative polymerase chain reaction.[44] Primers used for quantifying total viral DNA were 5′-TGTGTGCCCGTCTGTTGTGT-3′ and 5′-GAGTCCTGCGTCGAGAGAGC-3′ and Taqman probe 5′-CGCCCGAACAGGGACTTGAA-3′. For 2LTR circles, the primers used were 5′-AACTAGAGATCCCTCAGACCCTTTT-3′ and 5′-CTTGTCTTCGTTGGGAGTGAATT-3′, and Taqman probe 5′-CTAGAGATTTTCCACACTGAC-3′.

In vivo *experiments.* All mice were handled according to procedures approved by the UK Home Office and the Imperial College London Research Ethics Committee. One-day-old MF1 mice were injected intramuscularly with 5 µl of each vector (four mice per group). Mice were killed at 1 and 3 months after injection and eGFP in muscle was visualized under a fluorescence stereomicroscope. For immunohistochemical staining, tibialis anterior muscle was fixed in paraformaldehyde and sections (5 µm) were cut from paraffin-embedded tissue blocks. Slides were placed in histoclear solution (R.A. Lamb, Eastbourne, UK), and then hydrated in graded ethanol solutions. Antigen retrieval was performed using sodium citrate buffer (2.94 g/l sodium citrate, pH 6) and heating. Endogenous peroxidase was blocked by incubation with 0.3% H_2O_2 (Sigma, Steinheim, Germany) in phosphate-buffered saline for 10 minutes. Slides were incubated with 2% normal mouse serum (Dako Cytomation, Glostrup, Denmark), then with avidin and biotin (Vector Laboratories, Peterborough, UK). Slides were incubated overnight with rabbit anti-GFP serum (A6455; Invitrogen, Paisley, UK), and then with biotinylated goat anti-rabbit secondary antibody (BA-1000; Vector Laboratories) for 40 minutes. After being thoroughly washed in phosphate-buffered saline, the slides were incubated with Vectastain ABC kit (Vector Laboratories, Burlingame, CA) in accordance with the manufacturer's instructions. AEC substrate (3-amino-9-ethylcarbazole; Vector Laboratories) was used for detecting peroxidase activity, in accordance with the manufacturer's instructions. Hematoxylin (Sigma, Gillingham, UK) was used for counterstaining and slides were then mounted in aquamount (BDH, Poole, UK). Images were obtained on a Leica DMLS upright microscope using a ×40 objective (Leica, Milton Keynes, UK) with a Canon Coolpix 4500 digital camera, and processed with Adobe Photoshop software for publication.

eGFP ELISA was performed for samples as described previously.[4] Briefly, the injected, green part of the muscle was excised and protein was extracted using a homogenizer (Griffiths tube; VWR, Lutterworth, UK) in lysis buffer (Reporter Gene Assay Lysis buffer; Roche, Welwyn Garden City). Total protein was assayed using Biorad reagent. eGFP was quantified in triplicate against a recombinant eGFP standard (Clontech, Mountain View, CA) using the monoclonal antibody ab1218-100 (1:10,000, ABcam) as primary antibody, and the monoclonal secondary antibody ab5688 (1:5,000, ABcam, Cambridge, UK). eGFP expression in the muscle was confirmed by comparing the ELISA results in muscle with those from the vector stocks (**Supplementary Table S1**). Total viral DNA was also extracted from the samples by homogenizing 50 mg of tissue and performing a salting-out method. Quantitative polymerase chain reaction was used for measuring the prevalence of 2LTR circles in the muscle samples.

Statistical analysis. Data from the integration efficiency quantification assays were analyzed using a Kuskal–Wallis test for statistical significance ($P < 0.05$), and particular groups were compared using a Mann–Whitney test. eGFP ELISA measurements were analyzed for statistical significance by the Kruskal–Wallis test.

ACKNOWLEDGMENTS

We wish to thank the Biotechnology and Biological Sciences Research Council, UK and Fundação para a Ciência e a Tecnologia, Portugal for funding. S.N.W. is funded by Philip Gray Fellowship awarded by the Katharine Dormandy Trust. A.J.T. is supported by the Wellcome Trust.

SUPPLEMENTARY MATERIAL

Table S1. eGFP protein was quantified from the viral stocks and from the 3 month muscle samples, using an eGFP ELISA.

REFERENCES

1. Naldini, L, Blomer, U, Gallay, P, Ory, D, Mulligan, R, Gage, FH *et al.* (1996). *In vivo* gene delivery and stable transduction of nondividing cells by a lentiviral vector. *Science* **272**: 263–267.
2. Kohn, DB, Sadelain, M and Glorioso, JC (2003). Occurrence of leukaemia following gene therapy of X-linked SCID. *Nat Rev Cancer* **3**: 477–488.
3. Lewinski, MK, Bisgrove, D, Shinn, P, Chen, H, Hoffmann, C, Hannenhalli, S *et al.* (2005). Genome-wide analysis of chromosomal features repressing human immunodeficiency virus transcription. *J Virol* **79**: 6610–6619.
4. Yanez-Munoz, RJ, Balaggan, KS, MacNeil, A, Howe, S, Smith, AJ, Buch, P *et al.* (2006). Effective gene therapy with non-integrating lentiviral vectors. *Nat Med* **12**: 348–353.
5. Nightingale, SJ, Hollis, RP, Pepper, KA, Petersen, D, Yu, XJ, Yang, C *et al.* (2006). Transient gene expression by nonintegrating lentiviral vectors. *Mol Ther* **13**: 1121–1132.
6. Brown, PO, Bowerman, B, Varmus, HE and Bishop, JM (1989). Retroviral integration: structure of the initial covalent product and its precursor, and a role for the viral IN protein. *Proc Natl Acad Sci USA* **86**: 2525–2529.
7. Varmus (1989). Retroviral virions and genomes. In: Howe, B (ed.) *Retroviruses*. American Society for Microbiology: Washington, DC.
8. Pang, S, Koyanagi, Y, Miles, S, Wiley, C, Vinters, HV and Chen, IS (1990). High levels of unintegrated HIV-1 DNA in brain tissue of AIDS dementia patients. *Nature* **343**: 85–89.
9. Pauza, CD, Galindo, JE and Richman, DD (1990). Reinfection results in accumulation of unintegrated viral DNA in cytopathic and persistent human immunodeficiency virus type 1 infection of CEM cells. *J Exp Med* **172**: 1035–1042.
10. Robinson, HL and Zinkus, DM (1990). Accumulation of human immunodeficiency virus type 1 DNA in T cells: results of multiple infection events. *J Virol* **64**: 4836–4841.
11. Cara, A and Reitz, MS Jr. (1997). New insight on the role of extrachromosomal retroviral DNA. *Leukemia* **11**: 1395–1399.
12. Panganiban, AT and Temin, HM (1983). The terminal nucleotides of retrovirus DNA are required for integration but not virus production. *Nature* **306**: 155–160.
13. Stevenson, M, Haggerty, S, Lamonica, CA, Meier, CM, Welch, SK and Wasiak, AJ (1990). Integration is not necessary for expression of human immunodeficiency virus type 1 protein products. *J Virol* **64**: 2421–2425.
14. Wu, Y (2004). HIV-1 gene expression: lessons from provirus and non-integrated DNA. *Retrovirology* **1**: 13.
15. Saenz, DT, Loewen, N, Peretz, M, Whitwam, T, Barraza, R, Howell, KG *et al.* (2004). Unintegrated lentivirus DNA persistence and accessibility to expression in nondividing cells: analysis with class I integrase mutants. *J Virol* **78**: 2906–2920.
16. Shoemaker, C, Goff, S, Gilboa, E, Paskind, M, Mitra, SW and Baltimore, D (1980). Structure of a cloned circular Moloney murine leukemia virus DNA molecule containing an inverted segment: implications for retrovirus integration. *Proc Natl Acad Sci USA* **77**: 3932–3936.

17. Li, L, Olvera, JM, Yoder, KE, Mitchell, RS, Butler, SL, Lieber, M *et al.* (2001). Role of the non-homologous DNA end joining pathway in the early steps of retroviral infection. *EMBO J* **20**: 3272–3281.
18. Farnet, CM and Haseltine, WA (1991). Circularization of human immunodeficiency virus type 1 DNA *in vitro*. *J Virol* **65**: 6942–6952.
19. Coffin, JM (1996). Retroviridae: the viruses and their replication. In: Fields, BN, Knipe, DM and PM Howely (eds) *Fields Virology.* Lippincott-Raven: Philadelphia, pp. 1767–1847.
20. Masuda, T, Kuroda, MJ and Harada, S (1998). Specific and independent recognition of U3 and U5 att sites by human immunodeficiency virus type 1 integrase *in vivo*. *J Virol* **72**: 8396–8402.
21. Zhou, H, Rainey, GJ, Wong, SK and Coffin, JM (2001). Substrate sequence selection by retroviral integrase. *J Virol* **75**: 1359–1370.
22. Zhu, K, Dobard, C and Chow, SA (2004). Requirement for integrase during reverse transcription of human immunodeficiency virus type 1 and the effect of cysteine mutations of integrase on its interactions with reverse transcriptase. *J Virol* **78**: 5045–5055.
23. Gallay, P, Hope, T, Chin, D and Trono, D (1997). HIV-1 infection of nondividing cells through the recognition of integrase by the importin/karyopherin pathway. *Proc Natl Acad Sci USA* **94**: 9825–9830.
24. Leavitt, AD, Robles, G, Alesandro, N and Varmus, HE (1996). Human immunodeficiency virus type 1 integrase mutants retain *in vitro* integrase activity yet fail to integrate viral DNA efficiently during infection. *J Virol* **70**: 721–728.
25. Cereseto, A, Manganaro, L, Gutierrez, MI, Terreni, M, Fittipaldi, A, Lusic, M *et al.* (2005). Acetylation of HIV-1 integrase by p300 regulates viral integration. *EMBO J* **24**: 3070–3081.
26. Johnson, AA, Santos, W, Pais, GC, Marchand, C, Amin, R, Burke, TR Jr. *et al.* (2006). Integration requires a specific interaction of the donor DNA terminal 5′-cytosine with glutamine 148 of the HIV-1 integrase flexible loop. *J Biol Chem* **281**: 461–467.
27. Brown, HE, Chen, H and Engelman, A (1999). Structure-based mutagenesis of the human immunodeficiency virus type 1 DNA attachment site: effects on integration and cDNA synthesis. *J Virol* **73**: 9011–9020.
28. Engelman, A (1999). *In vivo* analysis of retroviral integrase structure and function. *Adv Virus Res* **52**: 411–426.
29. Esposito, D and Craigie, R (1998). Sequence specificity of viral end DNA binding by HIV-1 integrase reveals critical regions for protein-DNA interaction. *EMBO J* **17**: 5832–5843.
30. Gerton, JL, Ohgi, S, Olsen, M, DeRisi, J and Brown, PO (1998). Effects of mutations in residues near the active site of human immunodeficiency virus type 1 integrase on specific enzyme-substrate interactions. *J Virol* **72**: 5046–5055.
31. Lu, R, Limon, A, Ghory, HZ and Engelman, A (2005). Genetic analyses of DNA-binding mutants in the catalytic core domain of human immunodeficiency virus type 1 integrase. *J Virol* **79**: 2493–2505.
32. Topper, M, Luo, Y, Zhadina, M, Mohammed, K, Smith, L and Muesing, MA (2007). Posttranslational acetylation of the human immunodeficiency virus type 1 integrase carboxyl-terminal domain is dispensable for viral replication. *J Virol* **81**: 3012–3017.
33. Philippe, S, Sarkis, C, Barkats, M, Mammeri, H, Ladroue, C, Petit, C *et al.* (2006). Lentiviral vectors with a defective integrase allow efficient and sustained transgene expression *in vitro* and *in vivo*. *Proc Natl Acad Sci USA* **103**: 17684–17689.
34. Vargas, J Jr., Gusella, GL, Najfeld, V, Klotman, ME and Cara, A (2004). Novel integrase-defective lentiviral episomal vectors for gene transfer. *Hum Gene Ther* **15**: 361–372.
35. Butler, SL, Hansen, MS and Bushman, FD (2001). A quantitative assay for HIV DNA integration *in vivo*. *Nat Med* **7**: 631–634.
36. Terskikh, AV, Ershler, MA, Drize, NJ, Nifontova, IN and Chertkov, JL (2005). Long-term persistence of a nonintegrated lentiviral vector in mouse hematopoietic stem cells. *Exp Hematol* **33**: 873–882.
37. Gregory, LG, Waddington, SN, Holder, MV, Mitrophanous, KA, Buckley, SM, Mosley, KL *et al.* (2004). Highly efficient EIAV-mediated *in utero* gene transfer and expression in the major muscle groups affected by Duchenne muscular dystrophy. *Gene Ther* **11**: 1117–1125.
38. Li, S, Kimura, E, Fall, BM, Reyes, M, Angello, JC, Welikson, R *et al.* (2005). Stable transduction of myogenic cells with lentiviral vectors expressing a minidystrophin. *Gene Ther* **12**: 1099–1108.
39. Demaison, C, Parsley, K, Brouns, G, Scherr, M, Battmer, K, Kinnon, C *et al.* (2002). High-level transduction and gene expression in hematopoietic repopulating cells using a human immunodeficiency [correction of imunodeficiency] virus type 1-based lentiviral vector containing an internal spleen focus forming virus promoter. *Hum Gene Ther* **13**: 803–813.
40. Zufferey, R, Dull, T, Mandel, RJ, Bukovsky, A, Quiroz, D, Naldini, L *et al.* (1998). Self-inactivating lentivirus vector for safe and efficient *in vivo* gene delivery. *J Virol* **72**: 9873–9880.
41. Dull, T, Zufferey, R, Kelly, M, Mandel, RJ, Nguyen, M, Trono, D *et al.* (1998). A third-generation lentivirus vector with a conditional packaging system. *J Virol* **72**: 8463–8471.
42. Burns, JC, Friedmann, T, Driever, W, Burrascano, M and Yee, JK (1993). Vesicular stomatitis virus G glycoprotein pseudotyped retroviral vectors: concentration to very high titer and efficient gene transfer into mammalian and nonmammalian cells. *Proc Natl Acad Sci USA* **90**: 8033–8037.
43. Miller, SA, Dykes, DD and Polesky, HF (1988). A simple salting out procedure for extracting DNA from human nucleated cells. *Nucleic Acids Res* **16**: 1215.
44. Kilzer, JM, Stracker, T, Beitzel, B, Meek, K, Weitzman, M and Bushman, FD (2003). Roles of host cell factors in circularization of retroviral DNA. *Virology* **314**: 460–467.